Salt intake induces epithelial-to-mesenchymal transition of the peritoneal membrane in rats.

Anneleen Pletinck[1], Claudia Consoli[2], Maria Van Landschoot[1],Sonja Steppan[3], Nick Topley[2], Jutta Passlick-Deetjen[4], Raymond Vanholder[1], Wim Van Biesen[1].

[1]Renal Division, Department of Internal Medicine, Gent University Hospital, Gent, Belgium

[2]Institute of Nephrology, Wales College of Medicine, Cardiff, UK

[3]Fresenius Medical Care Germany, Bad Homburg, Germany

[4]Department of Nephrology, Heinrich-Heine University, Düsseldorf, Germany

Correspondence:

Wim Van Biesen, MD, PhD

Renal Division, Department of Internal Medicine

University Hospital Ghent

De Pintelaan 185

9000 Ghent

Belgium

fax: 0032 9 2404599

e-mail: wim.vanbiesen@ugent.be

Running title: Dietary salt intake and EMT.

ABSTRACT

Background.

Dietary salt intake has been linked to hypertension and cardiovascular disease through volume - mediated effects. Accumulating evidence points to direct negative influence of salt intake independent of volume overload, such as cardiac and renal fibrosis, mediated through transforming growth factor beta (TGF-β). Epithelial-to-mesenchymal transition (EMT) has been implicated as a key process in chronic fibrotic diseases, such as chronic kidney disease or heart failure. The potential role of dietary salt intake on cell transdifferentiation has never been investigated. This study analysed the effect of dietary salt intake on EMT and fibrosis in the peritoneal membrane (PM) in a rat model.

Methods.

Twenty-eight Wistar rats were randomized to a normal salt (NS) or a high salt (HS) intake. NS and HS rats had free access to tap water or NaCl 2% as drinking water, respectively. After 2 weeks, samples of peritoneum were taken, and TGF-β_1, Interleukin 6 (IL-6) and vascular endothelial growth factor (VEGF) mRNA expression were quantified with qRT-PCR. Fibrosis and submesothelial PM thickness were scored. EMT was evaluated using fluorescence staining with cytokeratin and alpha-smooth muscle actin (α-SMA).

Results.

Dietary salt intake caused peritoneal fibrosis and thickening of the submesothelial layer and induced EMT as identified by co-localization of cytokeratin and α-SMA in cells present in the submesothelial layer. Peritoneal TGF-β_1 and IL-6 mRNA expression were upregulated in the HS group.

Conclusion.

High dietary salt intake induces EMT and peritoneal fibrosis, a process coinciding with upregulation of TGF-β1.

KEYWORDS

epithelial-to-mesenchymal transition

IL-6

peritoneal membrane

salt

TGF-β_1

SHORT SUMMARY

This paper demonstrates that a high dietary salt intake on itself can result in epithelial-to-mesenchymal transition and fibrosis of the peritoneal membrane. This is of direct clinical relevance, as it could explain why already before peritoneal dialysis is started, differences in peritoneal membrane quality can be found. Dietary salt restriction is thus of importance in patients with chronic kidney disease, even during the pre-dialysis episode.

Introduction

Salt has been linked to hypertension since many years.[1;2] Initially it was thought that mainly the volume overload, induced by salt retention, was the underlying mechanism and that this in turn was the driving factor for left ventricular hypertrophy. Recently, there is accumulating evidence that dietary salt intake by itself, even without causing hypertension or volume overload, might be deleterious, and results in cardiac remodelling, fibrosis and left ventricular hypertrophy.[3;4] Also in the kidney, it has been demonstrated that salt intake leads to enhanced glomerulosclerosis and deterioration of residual renal function.[5-7] It has been postulated that upregulation of transforming growth factor beta 1 (TGF-β_1) might be one of the underlying mechanisms. The effects of TGF-β_1 seem to be diminished in the presence of nitric oxide (NO),[5] implying that salt - mediated upregulation of TGF-β_1 might be even more deleterious in subjects with NO deficiency,[8] such as in uremia[3]. TGF-β is a potent inducer of epithelial-to-mesenchymal transition (EMT),[9;10] a process which has recently been linked to chronic fibrotic diseases, such as chronic kidney disease, heart failure, lung and hepatic fibrosis.[11-15] In these diseases, EMT results in transdifferentiation of epithelial cells to myofibroblasts, which invade the interstitial space by transgression of the basal membrane, and expand the extracellular matrix. The link between dietary salt intake and cellular transdifferentiation has, to our knowledge, never been investigated.

In long - term peritoneal dialysis (PD) patients, both functional[16;17] and morphological[18;19] deterioration of the PM have been described. The morphological changes consist of neo-vascularisation, fibrosis[19] and EMT[20]. These negative effects have been related to exposure to glucose and glucose degradation products contained in the peritoneal dialysate, and to uraemia *per se.*[16;21;22] TGF-β_1 has been linked to glucose - induced enhanced senescence of mesothelial cells,[23] peritoneal fibrosis, and induction of EMT in the PM.[24;25] De Vriese et al[21] have demonstrated that interaction of advanced glycation end products (AGE) with their cell surface receptor for AGE (AGE-RAGE interaction) in uremia induces upregulation of TGF-β_1,

a process which they could also link to EMT. The role of dietary sodium intake on the deterioration of the PM has however never been investigated. It is conceivable that patients who have a high dietary salt intake will also need more hypertonic glucose exchanges, because they will drink more. In addition, if high salt intake would lead to upregulation of TGF-β_1 in the PM, in parallel to what has been shown for the heart and the kidneys, or an upregulation of vascular endothelial growth factor (VEGF), leading to neoangiogenesis like has been shown in the PM of PD patients, this would result in synergistic mechanisms leading to a rapid deterioration of the PM.

The present study has been undertaken to explore the effects of dietary salt loading on the PM in normal rats, with specific focus on EMT and fibrosis, and the role of TGF-β_1, VEGF and interleukin 6 (IL-6).

MATERIALS AND METHODS

Laboratory animals

Experiments were performed in 28 female Wistar rats (Iffa Credo, Brussels, Belgium), receiving care in accordance with the national guidelines for care and use of laboratory animals. The protocol was approved by the Ethical Committee of Experimental Animal Studies at the Faculty of Medicine and Health Sciences, Ghent University, Belgium.

Study Protocol

The rats were randomly assigned to two groups: NS (normal salt intake) and HS (high salt intake). Each group was housed in separate cages. The NS group received normal rat chew (rat and mice maintenance chew, Carfil, Oud-Turnhout, Belgium) with a 0.1% salt content, and free access to tap water. The HS group received the same rat chew, but had only free access to NaCl 2% as drinking water. Rats were weighed daily. After 2 weeks, rats were sacrificed. They were anaesthetized with thiobutabarbital (Inactin®,100mg/kg s.c., Sigma, St.Louis, MO). The trachea was intubated to facilitate breathing, a carotid artery was cannulated for monitoring of arterial blood pressure and the abdomen was opened by a midline incision for tissue sampling. Samples of visceral peritoneum (VP) and parietal peritoneum (PP) were immediately fixed in a 4% phosphate buffered formaldehyde solution (pH=7) (Klinipath, Olen, Belgium) and embedded in paraffin. The VP of the small and large bowel was entirely resected and together with biopsies of the PP, snapped frozen in liquid nitrogen and maintained at - 80°C until analysis.

(Immuno)histochemistry

From all tissue samples, 5-µm sections were cut with a Leica RM 2145 sliding microtome (Leica Microsystems, Nussloch, Germany) for histology and immunohistochemistry. A Sirius Red staining (Klinipath, Geel, Belgium) was used to evaluate fibrosis in the VP. Sections of the VP were deparaffinized, rehydrated and stained with Giemsa. Subsequently, sections were washed and stained with 0.1% Sirius Red, resulting in a brick red staining of all fibrillary collagen. To determine the thickness of the PP, the sections were sliced perpendicularly to the peritoneal surface, and a classic Masson's trichome staining was performed. Sections of the PP were deparaffinized, rehydrated and stained with Haematoxylin Gill (Merck, Brussels, Belgium). Successively, sections went through a series of fluids [1% HCl (VWR, Leuven, Belgium), a ponceau (Sigma, Bornem, Belgium)-fuschin (VWR) mixture, phosphomolybdene acid and anilin blue (VWR)] to obtain the desired colour.

Immunofluorescence stainings for alpha smooth muscle actin (α-SMA) and cytokeratin, as well as a double staining, were performed. Sections of VP were deparaffinized, rehydrated and pre-treated for antigen retrieval in Tris/EDTA (Tris[hydroxymethyl]aminomethane and [Ethylenedinitrilo]tetraacetic acid) (Acros Organics, Geel, Belgium) epitope retrieval solution (pH 9.0) at 96°C for 30 minutes. After cooling down, free aldehyde groups were blocked with NH_4Cl to block cross-linking of the antibodies (Ab) to inappropriate structures, and 1% BSA /TBS was used to block aspecific binding of the Ab. Subsequently, sections were incubated with the primary antibody: either a mouse monoclonal anti-human α-SMA Ab (M0851, Dako, Heverlee, Belgium) and/or a polyclonal rabbit anti-cow cytokeratin Ab (Z0622, Dako), followed respectively by a secondary goat anti-mouse Ab labelled with a green fluorecent dye (A-11017, Invitrogen, Merelbeke, Belgium) and/or a goat anti-rabbit Ab labelled with a red fluorescent dye (A-11072, Invitrogen). Sections were incubated shortly with a DAPI nuclear stain (Invitrogen) and finally mounted with Vectashield mounting medium (Labconsult, Brussels, Belgium).

Morphometric analysis

Morphometric measurements of the stainings were made by a blinded operator with an Olympus BX41 microscope (Olympus, Aartselaar, Belgium) at magnification x400. From each experimental animal, three peritoneal samples were analysed. For each sample, three sections were analysed quantitatively with a computerized image analysis system (CellD software,Olympus). For the Sirius Red staining, the total amount of connective tissue (%) in the VP was determined. For the Masson's trichome staining, the thickness of the PP was measured. The double α-SMA/cytokeratin staining was viewed with a fluorescence microscope (Axioscoop, Zeiss, Germany) and pictures were taken, using CellF Software (Olympus Soft Imaging Solutions, Germany). A semi-quantitative assessment was performed independently by two blinded operators. Each section was screened to estimate the extent and distribution of colocalization of α-SMA and cytokeratin. Staining results were classified from 0 to 3: 0=no, 1=mild-, 2=moderate- and 3=pronounced colocalization and migration of mesothelial cells into the interstititium. The results were calculated as the mean of the individual scores of the two operators for each sample.

IL-6/TGF-β_1/VEGF mRNA determination

Tissues were homogenized in TRI-Reagent (AB, Applied Biosystems, Foster City, CA, USA) on ice using a PowerGen 125 Tissue Homogenizer (Fisher Scientific). An aliquot of homogenate was separated into aqueous and organic phases by chloroform (Sigma) addition and centrifugation. RNA was precipitated from the aqueous phase by addition of isopropanol (Sigma), washed with ethanol (MERCK) and solubilized. Concentration and purity of the extracted RNA were determined by spectrophotometry (UV-DU64 spectrophotometer, Beckman). Each sample was confirmed for integrity using the Agilent 2100 BioAnalyzer (Agilent Technologies, Santa Clara, CA, USA). Reverse transcription was

performed by using the High Capacity cDNA Reverse Transcription kit (AB). Thermal cycling conditions were 25°C (10'), 37°C (120'), 85°C (5'') and 4°C (∞). All cDNA samples were stored at -20°C until analysis. The expression of IL-6, TGF-β_1 and VEGF mRNA was quantified by using the 7900HT Fast Real Time PCR System (AB). The thermal profile consisted of two hold steps, one at 50°C (2') and one at 95°C (10'), followed by 40 cycles x[95°C (15''), 60°C (1')]. RT - PCR efficiencies for each assay were calculated using the formula: Efficiency = $[10_{(1/slope)}] - 1$. Samples and endogenous control were amplified in separate wells in a 96-well-plate. The samples were run in triplicate and normalized to actin glyceraldehyde-3-phosphate dehydrogenase (GAPDH) levels, which was used as the endogenous control (reference gene). Pre-designed and labelled primer/probe sets were purchased from AB (TaqMan® Gene Expression Assays). The relative expression compares mRNA expression levels of the genes of interest (GOI; IL-6, TGF-β_1, VEGF) to the expression levels of the endogenous reference gene (Ref; GAPDH) according to the$\Delta\Delta$Ct method. In this method, the cycle in which the fluorescence level crosses a threshold value of fluorescence, during the exponential phase of amplification, is determined. As the fluorescence is directly correlated to the amount of double-stranded DNA present in each amplification cycle, the number of cycles needed to reach this level can therefore be used to calculate relative amounts of starting transcript mRNA. These values are expressed as relative values to an endogenous reference (=an internal control gene) to correct for differences in transcription rate and sample size between animals. Normalized relative quantity (NRQ) values were calculated using the following formula, as described previously by M.W.Pfaffl[26]:

$$NRQ = \frac{(E_{target})^{\Delta Ct_{target}(control-sample)}}{(E_{ref})^{\Delta Ct_{ref}(control-sample)}}$$

NRQ-values from HS rats were compared to those from NS rats, and expressed as relative increases (fold increase) between groups.

Statistical Analysis

Data analysis was performed with SPSS version 15.0 (SPSS Inc, Chicago, USA). Normal distribution of data was tested using Kolmogorov - Smirnov testing. Data are accordingly presented as mean ± standard deviation (SD). Normally distributed data were compared with the Student's *t*-test for independent samples. P-values < 0.05 (two-tailed probability) were considered as significant. The increase in relative mRNA expression between NS and HS was calculated, and 95% confidence intervals (CI) were determined. Hereto, the natural log transformation of the NRQ was calculated, the difference of the mean between the test group and the control group was calculated, and this value was used as the exponent of 2, resulting in the fold increase with its corresponding 95% CI. For the NS group, data of the NS were used both for test and control, which theoretically should result in a mean difference of zero, and thus a 1-fold increase in mRNA expression.

RESULTS

General data of laboratory animals (table 1)

Mean body weight of the rats was 213±7 g. After 2 weeks, rats of the HS group had a lower weight, compared with the rats of the NS group. Blood pressure after 2 weeks was not different between the HS and NS groups. Haematocrit levels were significantly lower in the HS group after 2 weeks. Mean daily water intake in the HS group was 62.5ml/rat, resulting in an extra dietary salt load of 1.25g/day/rat.

Peritoneal morphology

Sirius Red staining of collagen was significantly more pronounced in the HS rats than in the NS rats. This was evident both in the submesothelial compact zone as in the interstitial tissue (18.8 ± 3.5 vs 24.7 ± 5.8 % of total tissue in the NS vs HS group, respectively; $P < 0.01$) (Figures 1 and 2). The Masson's Trichome staining showed a significant thickening of the submesothelial layer of PP in the HS group (13.7 ± 3.2 vs 18.7 ± 3.7 µm in the NS vs HS group, respectively; $P < 0.001$) (Figures 3 and 4). Staining for the epithelial marker cytokeratin was confined to the mesothelial cell layer in all NS animals. In the HS animals, an extensive additional staining was observed in the submesothelial tissue. Staining for α-SMA was limited to the muscularis of the blood vessels in all the NS rats, but was also found in submesothelial areas in HS rats (Figure 5). Double α-SMA/cytokeratin staining with fluorescence was virtually absent in all the NS animals, but was significantly prominent in HS animals (score 0.25 ± 0.25 vs 1.22 ± 0.32 in the NS vs HS group, respectively; $P < 0.001$) (Figure 6).

mRNA expression of IL-6, TGF-β_1 and VEGF

Expression of IL-6 mRNA was upregulated 4.25 (95% CI: 2.22-8.13) times in the HS versus the NS group in the VP, and 1.94 (95% CI: 1.37-2.75) times in the PP.

Expression of TGF-β_1 mRNA was upregulated 2.10 (95% CI: 1.31- 3.37) times in the HS vs the NS group in the VP, and 1.32 (95% CI: 1.08-1.60) times in the PP. Expression of VEGF mRNA was not upregulated in the VP nor in the PP (Figure 7).

DISCUSSION

This study demonstrates that dietary salt intake by itself induces EMT of mesothelial cells as identified by co-localization of cytokeratin and α-SMA in the submesothelial layer, and fibrosis of the PM as documented by Sirius Red staining, and a thickening of the submesothelial layer on Masson's trichrome staining. Concordant with this, peritoneal TGF-β_1 and IL-6 mRNA expression were increased, but not VEGF mRNA expression. These observations suggest that dietary salt loading induces EMT and peritoneal fibrosis, potentially by upregulation of TGF-β1 and IL-6 mRNA.

It is now progressively accepted that EMT underlies epithelial degeneration and fibrogenesis in some chronic degenerative, fibrotic disorders, in particular of the heart[15], the kidney[11], the lung[14] and the liver[13]. TGF-β_1 is able to induce all the basic steps of EMT: loss of epithelial adhesion properties, *de novo* α-SMA expression and actin reorganization, disruption of basement membrane and enhanced cell migration and invasion capacity.[27] Also in the PM, there are several lines of evidence that TGF-β_1 plays a pivotal role in EMT and enhanced fibrosis. Margetts *et al.* used an adenoviral vector to increase TGF-β_1 expression in a rat model of PD.[24] By day 28, a substantial thickening of the PM was observed. Further experiments indicated that overproduction of TGF-β_1 resulted in an increase in expression of genes associated with EMT and fibrosis, such as those regulating type I collagen A2, α-SMA, and the zinc finger regulatory protein Snail.[25] Seven to fourteen days after exposure to TGF-β_1, appearance of epithelial cells in the submesothelial zone could be demonstrated. This phase was associated with disruption of the basement membrane and increased expression of matrix metalloproteinase 2.

In our experiments, there was clear EMT of the peritoneal membrane in the rats fed with a high salt diet, as we observed colocalization of cytokeratin and α-SMA, as a hallmark of transdifferentiation of mesenchymal cells. In addition, these cells were localized in the submesothelial cell layer, as a sign of their transgression through the basal membrane with

beginning invasion of the extracellular matrix. To our knowledge, this is the first observation of a link between dietary salt intake and EMT of the peritoneal membrane.

So far, it is unclear how salt upregulates TGF-β_1 expression. Ying and Sanders suggested that salt-induced shear stress in glomeruli activates tetraethylammonium-sensitive potassium channels, resulting in enhanced TGF-β_1 production.[7] More recently, the same group demonstrated that dietary salt induces the activation of proline-rich tyrosine kinase-2 (Pyk2) and identified c-Src as an important binding partner of Pyk2 in dietary salt-mediated production of TGF-β_1. Their data support the hypothesis that activation of Pyk2 recruits and activates c-Src and that this complex participates integrally in the vascular production of TGF-β_1 in response to dietary salt in the rat.[28] Others have made a link with digitalis-like substances, such as marinobufagenin, which tends to be upregulated by salt loading[29;30] and results in enhanced formation of pro-collagen in the heart.[31] Digitalis-like substances block the Na/K-ATPase pumps, and thus increase the intracellular Ca^{2+} concentration, which can activate calcium-dependent and downstream pro-fibrotic pathways.

Angiotensin II stimulates extracellular matrix protein synthesis through induction of TGF-β in rat mesangial cells.[32] In addition, there is accumulating evidence that intracellular angiotensin II plays an important role in renal cellular growth and fibrotic responses by activating NF-κB signalling, which is also on the final common pathway of the TGF-β_1 pathway.[33] Several studies have demonstrated that high salt intake decreases circulating levels of angiotensin II, but activates the tissue renin-angiotensin-aldosterone system (RAAS).[34;35] In salt-sensitive rats, a high salt intake resulted in increased intrarenal RAAS activity, associated with renal hypertrophy, fibrosis and damage.[34] Liang and Leenen demonstrated that fibrosis under these conditions of salt loading and high intrarenal RAAS activity, could be prevented by ACE- inhibiting drugs.[35] This might explain why use of ACE-inhibitors has a positive impact on PM morphology.[36]

Another potential mechanism is that the creation of local hyperosmolarity in the gut activates a tonicity-responsive enhancer binding protein (TonEBP)-mediated response. TonEBP activates osmoprotective genes to ensure cell function in hostile environments with increased interstitial tonicity, such as the renal medulla[37] and the lymphatic system[38]. A recent paper[39] showed that high salt intake increases protein expression of e.g. VEGF in macrophages in the subcutaneous tissue through activation of TonEBP. If such an hyperosmolarity-driven response would exist in the gut, it would be conceivable that this can be one of the mechanisms of EMT and the changing peritoneal morphology during long-term PD, where the peritoneum is exposed to hypertonic solutions. Further elaboration of this exciting hypothesis is certainly warranted, as it would imply that changing glucose for another hyperosmolar osmotic agent will not avoid the long-term peritoneal damage observed during PD. Next to TGF-β_1, also IL-6 expression is linked to PM degeneration and fibrosis[40] and this was the case as well as in the present study. It is not clear how salt intake upregulates IL-6 expression. It might be that upregulation of TGF-β_1 leads to upregulation of IL-6. *In vitro* experiments already showed that TGF-β_1 can induce IL-6 production in human myoblasts in a dose- and time-dependent manner.[41] This finding is in agreement with studies which reports similar *in vitro* results in other cell types: TGF-β1 increases IL-6 mRNA levels in cultured thymus epithelial cells[42] and astrocytes,[43] and IL-6 protein secretion in bone marrow stromal cells.[44] A recent paper by Leung et al showed no clear association between upregulation of TGF-β and IL-6 in cultured HPMC's.[40] However, the subtle and complex interplay of different cell types *in vivo* cannot be completely mimicked *in vitro* with one single cell type. In our experiments, there was a slight upregulation of VEGF mRNA in the visceral, but not in the parietal membrane. This could point to a mechanism where the upregulation of TGF-β_1 and IL-6 induces upregulation of VEGF, as in the study by Margetts *et al.*,[45] rather than to a direct upregulation of VEGF by the enhanced dietary salt intake. Also here, upregulation of TonEBP by creation of a hypertonic environment in the gut, might be involved.[39]

Adipocytes are ubiquitous in peritoneal tissue and it is hypothesized that they can be an important source of cytokine secretion, including IL-6 and TGF-β.[46;47] In our study, salt intake induced a more pronounced upregulation of IL-6 and TGF-β_1 expression in the VP, where adipocytes are abundant, as compared to the PP, where less adipocytes are present.

Many experiments considering well-defined signalling pathways, e.g. in an *in vitro* setting, use purified stimulating factors in high concentrations, which does not represent the biological situation where a complex interplay of different pathways and cells is possible. In our model, the only intervention was an increased dietary salt intake, but nevertheless, the resulting effects on EMT were still as impressive.

Of course, the pathways leading to these observations need further elaboration. Potential interventions are the use of inhibitors of the renin-angiotensin system, of TGF-β1 and/or of TonEBP. Also the potential role of adipocytes and of macrophages infiltrating adipose tissue needs further exploration.

It is surprising that the effects of salt intake appeared so rapidly, after only 2 weeks of exposure. However, Ying and Sanders[7] also demonstrated enhanced renal fibrosis and glomerulosclerosis linked to upregulation of TGF-β after 15 days of salt loading in rats, and effects on the vasculature even after 4 days.[48] Machnik et al[39] found important changes in the subcutaneous tissue after 2 weeks of salt loading in rats. All these experiments point out that effects of high salt intake seem to appear very rapidly.

Finally, the question arises in how far our findings impact the application of PD which is a well-established renal replacement modality. Unfortunately, its longevity as a technique is restricted by functional and morphological deterioration of the PM over time.[16;18;19;49] It has always been puzzling why some patients do and others do not develop such morphological alterations. Although deterioration of the PM is mostly attributed to the exposure to PD fluids and peritonitis,[16;50-52] large differences in PM structure and function can be found already at

the start of PD, as is apparent both from morphological studies, such as the PD biopsy registry,[19] and from functional studies.[16;53] So far, this has been explained by differences in comorbidities such as diabetes, genetic background and/or uraemia.[54-56] Hence, the changes over time of the PM in PD patients are not exclusively induced by the exposure to PD fluids and inflammation. Our study adds dietary salt intake to the underlying mechanisms, even without exposure to PD fluids. This finding becomes even more relevant in view of the need for more hypertonic glucose, which by itself is damaging to the PM, to counter volume overload in the case of high salt intake, thus initiating a synergistic pathway to a faster deterioration of the PM. This synergism needs further investigation. As such, our findings of peritoneal fibrosis and EMT of mesothelial cells induced by dietary salt intake are of direct clinical relevance for patients on PD. Dietary salt restriction is thus of importance in patients with chronic kidney disease, even during the pre-dialysis phase.

In conclusion, dietary salt intake in non-uraemic rats induced eEMT and peritoneal fibrosis. This was correlated with an upregulation of TGF-β1 and IL-6 mRNA, which could be the link between dietary salt intake and EMT.

Acknowledgements.

The authors thank Julien Dupont and Marie-Anne Waterloos for their expert technical assistance and Liesbeth Ferdinande and Isabelle Rottiers for helping with the optimization of the staining protocols and the interpretation of the fluorescence stainings. We also thank Prof Jan De Bleecker for the use of the fluorescence microscope. The abstract of this paper has been presented as an oral presentation at the XLV Congress of the European Renal Association European Dialysis and Transplant Association, Stockholm, Sweden (May 10-13, 2008).

Conflict of interest.

The results presented in this paper have not been published previously in whole or part, except in abstract form. W.V.B. received speaker fees from Fresenius Medical Care, Baxter and Gambro. S.S. and J.P.-D. are employees of Fresenius Medical Care.

REFERENCES

1. Frohlich ED, Varagic J. The role of sodium in hypertension is more complex than simply elevating arterial pressure. *Nat Clin Pract Cardiovasc Med* 2004; 1: 24-30

2. Haddy FJ. Role of dietary salt in hypertension. *Life Sci* 2006; 79: 1585-1592

3. Ritz E, Dikow R, Morath C, Schwenger V. Salt--a potential 'uremic toxin'? *Blood Purif* 2006; 24: 63-66

4. Frohlich ED, Varagic J. Sodium directly impairs target organ function in hypertension. *Curr Opin Cardiol* 2005; 20: 424-429

5. Sanders PW. Salt intake, endothelial cell signaling, and progression of kidney disease. *Hypertension* 2004; 43: 142-146

6. Sanders PW. Effect of salt intake on progression of chronic kidney disease. *Curr Opin Nephrol Hypertens* 2006; 15: 54-60

7. Ying WZ, Sanders PW. Dietary salt modulates renal production of transforming growth factor beta in rats. *Am J Physiol* 1997; 274: 635-641

8. Chen PY, St John PL, Kirk KA, Abrahamson DR, Sanders PW. Hypertensive nephrosclerosis in the Dahl/Rapp rat. Initial sites of injury and effect of dietary L-arginine supplementation. *Lab Invest* 1993; 68: 174-184

9. Xu J, Lamouille S, Derynck R. TGF-beta-induced epithelial to mesenchymal transition. *Cell Res* 2009; 19: 156-172

10. Zavadil J, Bottinger EP. TGF-beta and epithelial-to-mesenchymal transitions. *Oncogene* 2005; 24: 5764-5774

11. Iwano M, Plieth D, Danoff TM, Xue C, Okada H, Neilson EG. Evidence that fibroblasts derive from epithelium during tissue fibrosis. *J Clin Invest* 2002; 110: 341-350

12. Liu Y. Epithelial to mesenchymal transition in renal fibrogenesis: pathologic significance, molecular mechanism, and therapeutic intervention. *J Am Soc Nephrol* 2004; 15: 1-12

13. Meindl-Beinker NM, Dooley S. Transforming growth factor-beta and hepatocyte transdifferentiation in liver fibrogenesis. *J Gastroenterol Hepatol* 2008; 23 Suppl 1: S122-S127

14. Willis BC, Borok Z. TGF-beta-induced EMT: mechanisms and implications for fibrotic lung disease. *Am J Physiol Lung Cell Mol Physiol* 2007; 293: L525-L534

15. Zeisberg EM, Tarnavski O, Zeisberg M *et al*. Endothelial-to-mesenchymal transition contributes to cardiac fibrosis. *Nat Med* 2007; 13: 952-961

16. Davies SJ, Phillips L, Naish PF, Russell GI. Peritoneal glucose exposure and changes in membrane solute transport with time on peritoneal dialysis. *Journal of the American Society of Nephrology* 2001; 12: 1046-1051

17. Heimbürger O, Waniewski J, Werynski A, Tranaeus A, Lindholm B. Peritonal transport in CAPD patients with permanent loss of ultrafiltration capacity. *Kidney International* 1990; 38: 495-506

18. Williams JD, Craig KJ, Topley N *et al*. Morphologic changes in the peritoneal membrane of patients with renal disease. *J Am Soc Nephrol* 2002; 13: 470-479

19. Williams JD, Craig KJ, Von RC, Topley N, Williams GT. The natural course of peritoneal membrane biology during peritoneal dialysis. *Kidney Int Suppl* 2003; S43-S49

20. Yanez-Mo M, Lara-Pezzi E, Selgas R *et al*. Peritoneal dialysis and epithelial-to-mesenchymal transition of mesothelial cells. *N Engl J Med* 2003; 348: 403-413

21. De Vriese AS, Tilton RG, Mortier S, Lameire NH. Myofibroblast transdifferentiation of mesothelial cells is mediated by RAGE and contributes to peritoneal fibrosis in uraemia. *Nephrol Dial Transplant* 2006; 21: 2549-2555

22. Slater ND, Cope GH, Raftery AT. Mesothelial hyperplasia in response to peritoneal dialysis fluid: a morphometric study in the rat. *Nephron* 1991; 58: 466-471

23. Ksiazek K, Korybalska K, Jorres A, Witowski J. Accelerated senescence of human peritoneal mesothelial cells exposed to high glucose: the role of TGF-beta1. *Lab Invest* 2007; 87: 345-356

24. Margetts PJ, Kolb M, Galt T, Hoff CM, Shockley TR, Gauldie J. Gene transfer of transforming growth factor-beta1 to the rat peritoneum: effects on membrane function. *J Am Soc Nephrol* 2001; 12: 2029-2039

25. Margetts PJ, Bonniaud P, Liu L *et al*. Transient overexpression of TGF-{beta}1 induces epithelial mesenchymal transition in the rodent peritoneum. *J Am Soc Nephrol* 2005; 16: 425-436

26. Pfaffl MW. A new mathematical model for relative quantification in real-time RT-PCR. *Nucleic Acids Res* 2001; 29: e45

27. Yang J, Liu Y. Dissection of key events in tubular epithelial to myofibroblast transition and its implications in renal interstitial fibrosis. *Am J Pathol* 2001; 159: 1465-1475

28. Ying WZ, Aaron K, Sanders PW. Mechanism of dietary salt-mediated increase in intravascular production of TGF-beta1. *Am J Physiol Renal Physiol* 2008; 295: F406-F414

29. Bagrov AY, Fedorova OV, Dmitrieva RI, French AW, Anderson DE. Plasma marinobufagenin-like and ouabain-like immunoreactivity during saline volume expansion in anesthetized dogs. *Cardiovasc Res* 1996; 31: 296-305

30. Fedorova OV, Lakatta EG, Bagrov AY. Endogenous Na,K pump ligands are differentially regulated during acute NaCl loading of Dahl rats. *Circulation* 2000; 102: 3009-3014

31. Elkareh J, Kennedy DJ, Yashaswi B *et al*. Marinobufagenin stimulates fibroblast collagen production and causes fibrosis in experimental uremic cardiomyopathy. *Hypertension* 2007; 49: 215-224

32. Zimpelmann J, Burns KD. Angiotensin-(1-7) activates growth-stimulatory pathways in human mesangial cells. *Am J Physiol Renal Physiol* 2009; 296: F337-F346

33. Zhuo JL, Li XC. Novel roles of intracrine angiotensin II and signalling mechanisms in kidney cells. *J Renin Angiotensin Aldosterone Syst* 2007; 8: 23-33

34. Bayorh MA, Ganafa AA, Emmett N, Socci RR, Eatman D, Fridie IL. Alterations in aldosterone and angiotensin II levels in salt-induced hypertension. *Clin Exp Hypertens* 2005; 27: 355-367

35. Liang B, Leenen FH. Prevention of salt induced hypertension and fibrosis by angiotensin converting enzyme inhibitors in Dahl S rats. *Br J Pharmacol* 2007; 152: 903-914

36. Kolesnyk I, Noordzij M, Dekker FW, Boeschoten EW, Krediet RT. A positive effect of AII inhibitors on peritoneal membrane function in long-term PD patients. *Nephrol Dial Transplant* 2009; 24: 272-277

37. Neuhofer W, Beck FX. Cell survival in the hostile environment of the renal medulla. *Annu Rev Physiol* 2005; 67: 531-555

38. Go WY, Liu X, Roti MA, Liu F, Ho SN. NFAT5/TonEBP mutant mice define osmotic stress as a critical feature of the lymphoid microenvironment. *Proc Natl Acad Sci U S A* 2004; 101: 10673-10678

39. Machnik A, Neuhofer W, Jantsch J *et al*. Macrophages regulate salt-dependent volume and blood pressure by a vascular endothelial growth factor-C-dependent buffering mechanism. *Nat Med* 2009; 15: 545-552

40. Leung JC, Chan LY, Tam KY *et al*. Regulation of CCN2/CTGF and related cytokines in cultured peritoneal cells under conditions simulating peritoneal dialysis. *Nephrol Dial Transplant* 2008;

41. Mazzarelli P, Scuderi F, Mistretta G, Provenzano C, Bartoccioni E. Effect of transforming growth factor-beta1 on interleukin-6 secretion in human myoblasts. *J Neuroimmunol* 1998; 87: 185-188

42. Schluns KS, Cook JE, Le PT. TGF-beta differentially modulates epidermal growth factor-mediated increases in leukemia-inhibitory factor, IL-6, IL-1 alpha, and IL-1 beta in human thymic epithelial cells. *J Immunol* 1997; 158: 2704-2712

43. Benveniste EN, Kwon J, Chung WJ, Sampson J, Pandya K, Tang LP. Differential modulation of astrocyte cytokine gene expression by TGF-beta. *J Immunol* 1994; 153: 5210-5221

44. Urashima M, Ogata A, Chauhan D *et al*. Transforming growth factor-beta1: differential effects on multiple myeloma versus normal B cells. *Blood* 1996; 87: 1928-1938

45. Margetts PJ, Oh KH, Kolb M. Transforming growth factor-beta: importance in long-term peritoneal membrane changes. *Perit Dial Int* 2005; 25 Suppl 3: S15-S17

46. Lai KN, Tang SC, Leung JC. Mediators of inflammation and fibrosis. *Perit Dial Int* 2007; 27 Suppl 2: S65-S71

47. Trayhurn P, Wood IS. Adipokines: inflammation and the pleiotropic role of white adipose tissue. *Br J Nutr* 2004; 92: 347-355

48. Ying WZ, Sanders PW. Dietary salt intake activates MAP kinases in the rat kidney. *FASEB J* 2002; 16: 1683-1684

49. De Vriese AS, Mortier S, Lameire NH. What happens to the peritoneal membrane in long-term peritoneal dialysis? *Perit Dial Int* 2001; 21 Suppl 3: S9-18

50. Davies SJ, Bryan J, Phillips L, Russell GI. Longitudinal changes in peritoneal kinetics: the effects of peritoneal dialysis and peritonitis. *Nephrol Dial Transplant* 1996; 11: 498-506

51. Mortier S, De Vriese AS, Van d, V, Schaub TP, Passlick-Deetjen J, Lameire NH. Hemodynamic effects of peritoneal dialysis solutions on the rat peritoneal membrane: role of acidity, buffer choice, glucose concentration, and glucose degradation products. *J Am Soc Nephrol* 2002; 13: 480-489

52. Mortier S, Faict D, Schalkwijk CG, Lameire NH, De Vriese AS. Long-term exposure to new peritoneal dialysis solutions: Effects on the peritoneal membrane. *Kidney Int* 2004; 66: 1257-1265

53. Van Biesen W, Carlsson O, Bergia R *et al*. Personal dialysis capacity (PDC(TM)) test: a multicentre clinical study. *Nephrol Dial Transplant* 2003; 18: 788-796

54. Gillerot G, Goffin E, Michel C *et al*. Genetic and clinical factors influence the baseline permeability of the peritoneal membrane. *Kidney Int* 2005; 67: 2477-2487

55. Stoenoiu MS, De Vriese AS, Brouet A *et al*. Experimental diabetes induces functional and structural changes in the peritoneum. *Kidney Int* 2002; 62: 668-678

56. Zareie M, De Vriese AS, Hekking LH *et al*. Immunopathological changes in a uraemic rat model for peritoneal dialysis. *Nephrol Dial Transplant* 2005; 20: 1350-1361

TABLE

Table 1. Characteristics of experimental animals

	Normal Salt n = 14	High Salt n = 14	p-value
Initial body weight (g)	211.9 ± 9.1	214.0 ± 5.9	P = NS
Body weight (g) after 2 weeks	234.9 ± 19.1	217.2 ± 11.5	P < 0.01
Blood pressure after 2 weeks (mmHg)	140.4 ± 22.0	137.5 ± 15.3	P = NS
Haematocrit level (%)	46.3 ± 1.7	44.2 ± 1.8	P < 0.01

LEGENDS TO FIGURES

Figure 1.

Sirius Red staining of collagen in the visceral peritoneal membrane (magnification x400). Prominent submesothelial and interstitial fibrosis was observed in the ‘high salt’ (C and D) animals compared with the ‘normal salt’ animals (A and B).

Figure 2.

The amount of connective tissue in the visceral peritoneal membrane was significantly different between the ‘normal salt’ (18.8 ± 3.5%) group and the ‘high salt’ (24.7 ± 5.8%) group ($P<0.01$). Data are expressed as mean ± SD for groups of 14 rats.

Figure 3.

Masson’s trichome staining of the parietal peritoneal membrane (magnification x400). The submesothelial thickness of the parietal peritoneum was increased in the ‘high salt’ (HS, panel B) group vs the normal salt group (NS, panel A).

Figure 4.

Submesothelial thickness of the parietal peritoneal membrane was significantly different between the ‘normal salt’ (13.7 ± 3.2 μm) group and the ‘high salt’ (18.7 ± 3.7 μm) group ($P<0.001$). Data are expressed as mean ± SD for groups of 14 rats.

Figure 5.

α-SMA-, cytokeratin- and a double staining for α-SMA and cytokeratin (magnification, x400). Serial sections of the visceral peritoneum from 'normal salt' (controls) rats (A-C) and 'high salt' rats (D-F) were stained for α-SMA (A,D,G), cytokeratin (B,E,H) and double stained for α-SMA and cytokeratin (C,F,I). In the control rats, only vascular smooth muscle cells stain for α-SMA (A), only mesothelial cells stain for cytokeratin (B) and virtually no α-SMA/cytokeratin colocalization (C) occurs. In the peritoneal membrane of the 'high salt' animals, α-SMA staining is found not only in the vascular smooth muscle layer of blood vessels, but also in submesothelial tissue (G). Cytokeratin staining (E) is visible in the mesothelial cells and is additionally found in the interstitial tissue. Co-localization of α-SMA and cytokeratin (F,I) is pronounced in submesothelial tissue. Thick arrow, colocalization.

Figure 6.

Semi-quantitative scoring for colocalization of α-SMA and cytokeratin. Double α-SMA/cytokeratin staining was virtually absent in the NS animals, but was significantly prominent in the HS animals (score 0.25 ± 0.25 vs 1.22 ± 0.32, in the NS vs HS group respectively, $P < 0.001$). Scoring was done by two independent blinded observers for three samples of each experimental animal as 0, no colocalization; 1, mild colocalization; 2, moderate colocalization; 3, strong colocalization.

Figure 7.

mRNA expression of IL-6, TGF-β_1 and VEGF: fold change high salt (HS) versus normal salt (NS). 'Normal salt' group = control group, taken as a standard. Fold change of the NS group = 1. In the 'high salt' group, expression of IL-6 mRNA was 4.25 times [CI: $(2.22, 8.13)_{HS}$ vs $(0.60, 1.65)_{NS}$] more upregulated in the visceral peritoneum (VP) and 1.94 times [CI: $(1.37, 2.75)_{HS}$ vs $(0.71, 1.39)_{NS}$] more upregulated in the parietal peritoneum (PP). TGF-β_1 mRNA expression was 2.1 times (CI: $[1.31, 3.37]_{HS}$ vs $[0.79, 1.26]_{NS}$) more upregulated in the VP and 1.32 times [CI: $(1.08, 1.60)_{HS}$ vs $(0.75, 1.31)_{NS}$] more upregulated in the PP. VEGF mRNA expression was 1.74 times [CI: $(0.97, 3.12)_{HS}$ vs $(0.81, 1.22)_{NS}$] higher in the VP, but was not different between the two groups in the PP [CI: $(0.84, 1.00)_{HS}$ vs $(0.83, 1.19)_{NS}$].

Figure 1

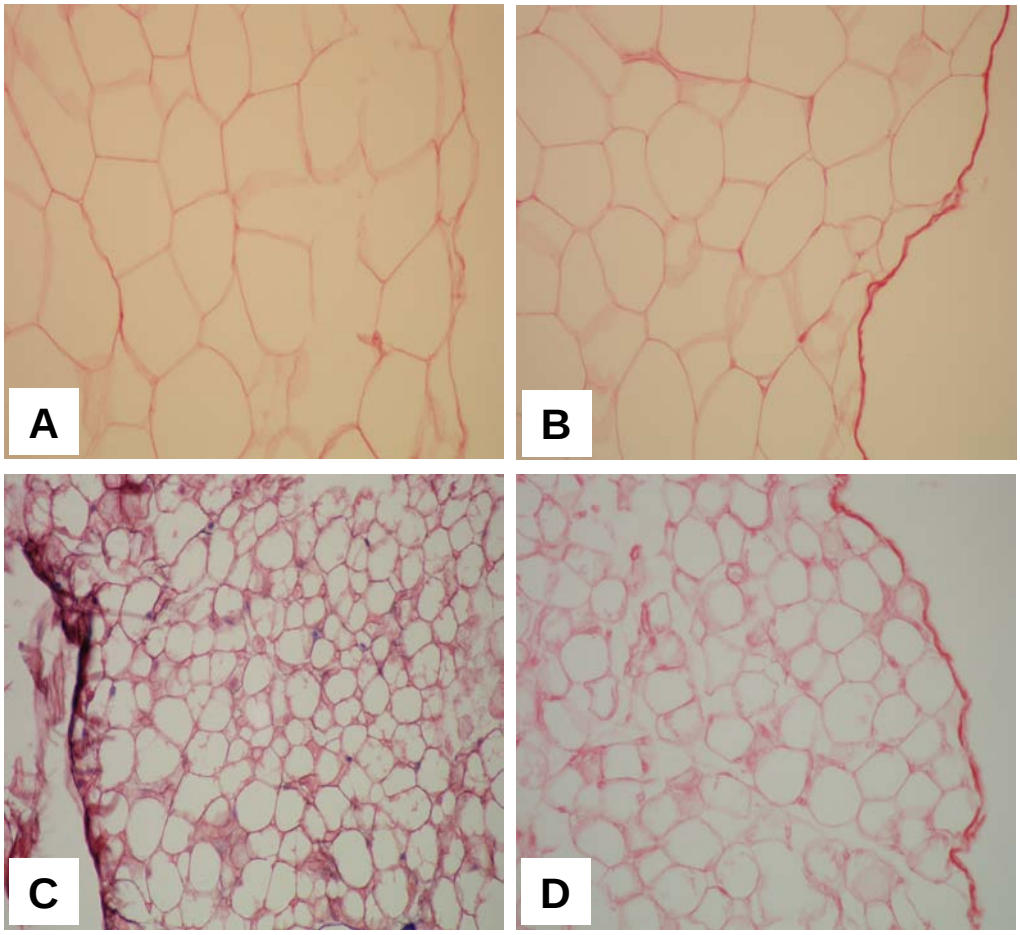

Figure 2

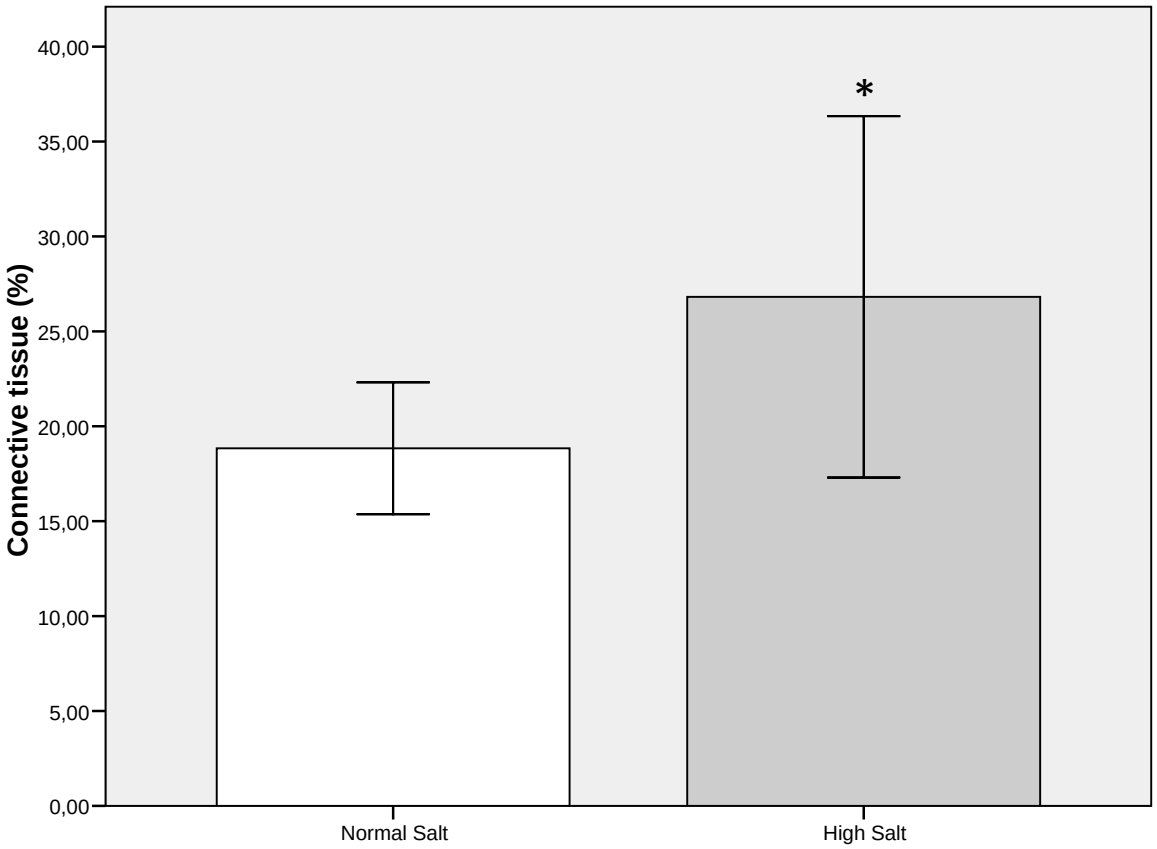

Error bars: +/- 1 SD

Figure 3

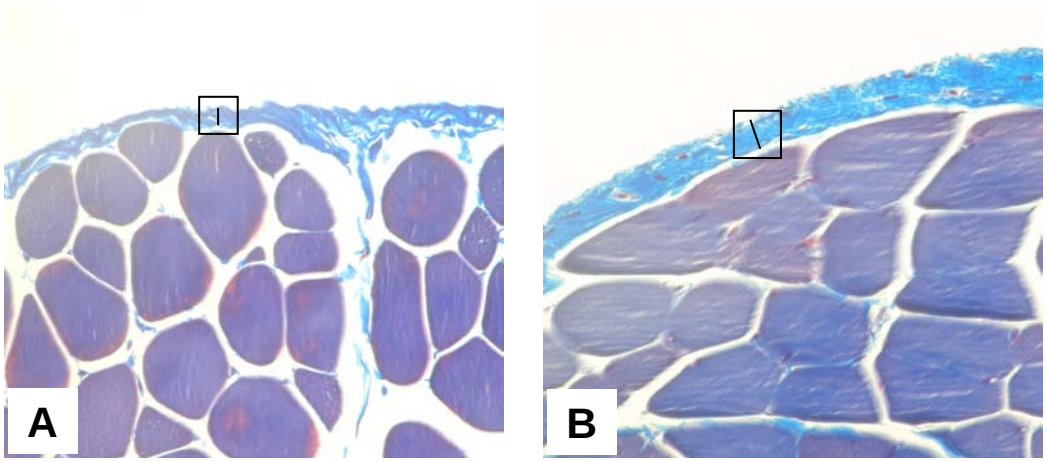

Figure 4

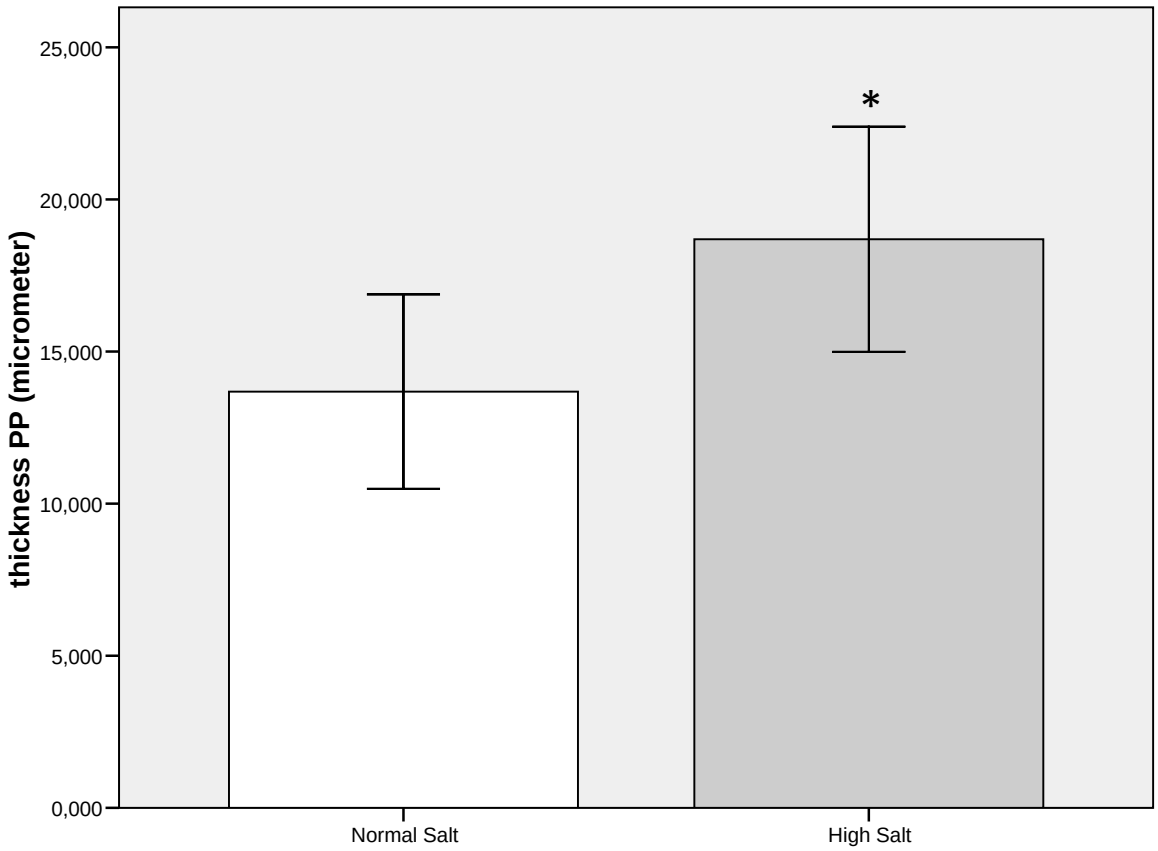

Error bars: +/- 1 SD

Figure 5

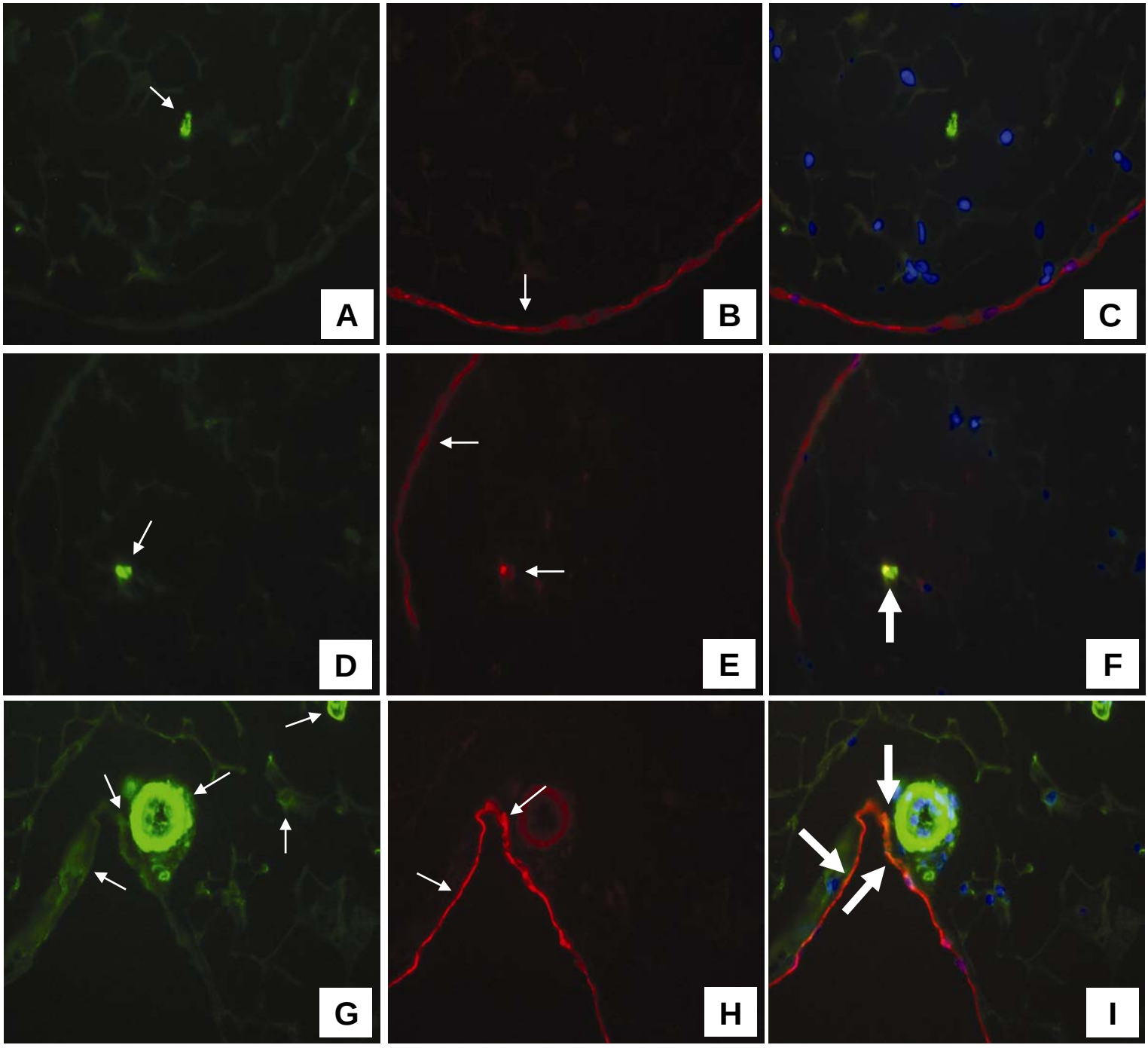

Figure 6

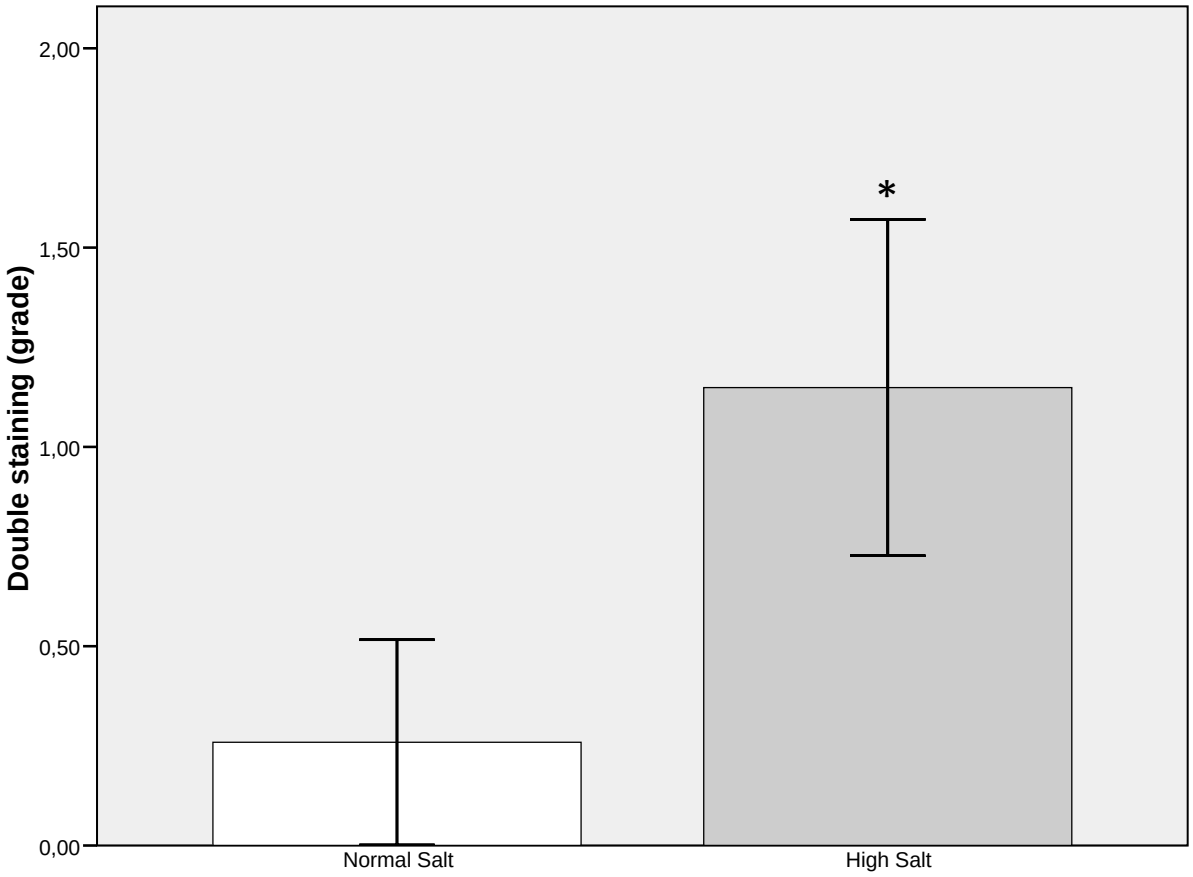

Error bars: +/- 1 SD

Figure 7

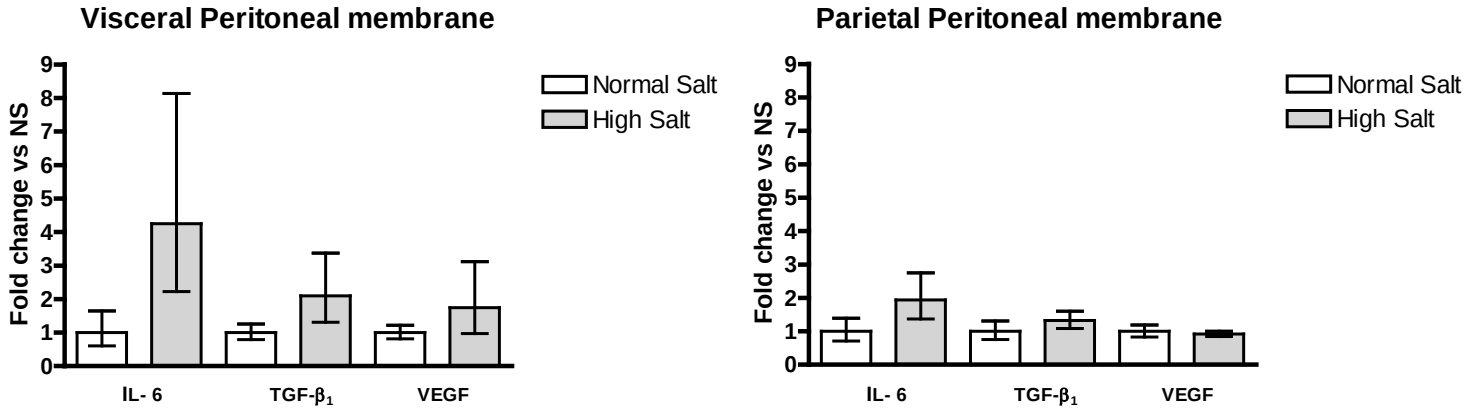
Visceral Peritoneal membrane
Fold change vs NS
0
1
2
3
4
5
6
7
8
9
IL- 6
TGF-β1
VEGF
Normal Salt
High Salt
Parietal Peritoneal membrane
Fold change vs NS
0
1
2
3
4
5
6
7
8
9
IL- 6
TGF-β1
VEGF
Normal Salt
High Salt